Microstructure to Substrate Self-Assembly Using Capillary Forces

Uthara Srinivasan, Dorian Liepmann, and Roger T. Howe, *Fellow, IEEE*

Abstract—We have demonstrated the fluidic self-assembly of micromachined silicon parts onto silicon and quartz substrates in a preconfigured pattern with submicrometer positioning precision. Self-assembly is accomplished using photolithographically defined part and substrate binding sites that are complementary shapes of hydrophobic self-assembled monolayers. The patterned substrate is passed through a film of hydrophobic adhesive on water, causing the adhesive to selectively coat the binding sites. Next, the microscopic parts, fabricated from silicon-on-insulator wafers and ranging in size from $150 \times 150 \times 15 \ \mu m^3$ to $400 \times 400 \times 50 \ \mu m^3$, are directed toward the substrate surface under water using a pipette. Once the hydrophobic pattern on a part comes into contact with an adhesive-coated substrate binding site, shape matching occurs spontaneously due to interfacial free energy minimization. In water, capillary forces of the adhesive hold the parts in place with an alignment precision of less than $0.2 \ \mu m$. Permanent bonding of the parts onto quartz and silicon is accomplished by activating the adhesive with heat or ultraviolet light. The resulting rotational misalignment is within $\sim 0.3°$. Using square sites, 98-part arrays have been assembled in less than 1 min with 100% yield. The general microassembly approach described here may be applied to parts ranging in size from the nano- to milliscale, and part and substrate materials including semiconductors, glass, plastics, and metals. [602]

I. INTRODUCTION

THE current "microengineering tool kit" is capable of producing a great range of sensor and actuator devices. This set of fabrication methods consists mainly of bulk and surface silicon micromachining, laser micromachining, and LIGA (the German acronym for X-ray lithography, electrodeposition, and molding). In the next generation of MEMS, micromechanical sensors and actuators will be integrated with electronic, optical, and fluidic components onto a variety of substrates to make powerful, complex microsystems [1]. At present, however, this remains a major challenge since the fabrication sequences and material requirements of the different components are often incompatible. The development of efficient wafer-scale assembly techniques can be used to overcome this hurdle and combine a variety of materials on a single chip.

"Pick and place" serial assembly techniques encounter speed and cost constraints in applications that require the assembly of large numbers of microscale components with high positioning precision [1]. In addition, surface forces must be carefully controlled to prevent unwanted adhesion of microscopic parts to each other or tool surfaces [2]. For these reasons, noncontact, parallel assembly techniques in which a large number of components may be assembled simultaneously with microscale precision are being developed. These microassembly processes generally fall into two categories—wafer-to-wafer transfer and self-assembly [1]. In the first route, microstructure transfer occurs between aligned wafers. The placement of structures is predetermined by the layout on the donor wafer, as in the work by Singh *et al.*, which employs compression bonding and cold welding between metal contacts [3]. Alternately, Holmes and Saidam have used laser-assisted release to position individual components on a target wafer in a different layout than on the donor grid by exposing the donor through a mask and moving both wafers accordingly [4].

In the self-assembly approach, a large number of microcomponents flows over a target substrate patterned with binding sites, and part-substrate attachment and alignment occur spontaneously due to free energy minimization. Because microscopic object handling and surface interactions are easier to control in a liquid environment, the majority of the processes being developed are fluidic. Self-assembly offers several compelling advantages over wafer-to-wafer transfer. This approach allows donor and target substrate layouts to be decoupled so expensive materials may be used most efficiently. In addition, self-assembly can reduce the yield losses associated with monolithic processes since the parts and substrates may be fabricated and tested separately, and defective elements may be discarded before the assembly step [1].

Various groups are developing self-assembly techniques at the microscale using different types of forces to achieve attraction and binding. A fluidic process that relies on gravitational and shear forces for self-assembly has been developed by Smith *et al.* [5]. In their approach, trapezoidally shaped microcomponents fill similarly shaped holes in a substrate. Since the planarity of the substrate is regained following assembly, electrical connections may be patterned after assembly using standard photolithographic techniques. This process has been used to assemble gallium arsenide light-emitting diodes onto silicon and silicon electronics onto glass for flat panel displays [5], [6]. The placement of tens of thousands of components per minute into arrays has been demonstrated with $\pm 1 \ \mu m$ precision, proving that fluidic self-assembly is a viable microassembly technique [6]. However, a drawback to using gravitational forces is that they are relatively weak compared to other forces at the microscale. This can cause difficulties in selectively removing in-

correctly assembled parts and cleaning the substrate once the assembly has been completed.

In other self-assembly work, Nakakubo and Shimoyama have used bridging flocculation and shape complementarity to bond microscale blocks to each other in a dilute polymer solution [7]. In the work of Murakami *et al.*, magnetic forces cause microscopic metal disks to attach onto a substrate patterned with arrays of nickel dots in water; while binding was observed, alignment did not occur [8]. In a dry approach, Cohn *et al.* have conducted feasibility experiments using electrostatic traps for self-assembly in vacuum with ultrasonic agitation to overcome friction and adhesion [9], [10].

To give high assembly yields as well as high positioning accuracy, it is important to employ not only relatively strong forces but also a lubrication strategy. Whitesides *et al.* have developed a procedure that fulfills these criteria using capillary forces and demonstrated the assembly of millimeter-scale plastic objects into aggregates and three-dimensional arrays [11]–[13]. Their technique involves a method of coating selected faces of the objects with thin lubricant films and agitating the objects in a second liquid medium (with which the lubricant is insoluble) so that the films on the binding faces can coalesce. The lubricant film and the medium are chosen so that the interface between the two has a high interfacial free energy, making it energetically favorable for the lubricant-coated faces to join and self-align to minimize the exposed lubricant-medium interfacial area. In [11], alkanes and photocurable methacrylates were used as lubricants due to their relatively high interfacial energies with water (approximately 50 mJ/m^2). Here, the binding faces of the plastic pieces were made hydrophobic, and the remaining surfaces were made hydrophilic. In their process, the hydrocarbon lubricant selectively coats only the hydrophobic binding faces under water, and the free energy of the lubricant-water interface is minimized upon assembly of two such surfaces. If a photocurable methacrylate is used as the lubricant, exposure to ultraviolet irradiation causes solidification of the adhesive layers after assembly and the aggregate can be removed from water.

Capillary forces are proportional to the length of the solid-liquid interface, and therefore decrease linearly with size [14], [15]. As a result, capillary forces become dominant relative to other forces (e.g., pressure and body forces, which are proportional to length^2 and length^3, respectively) as components are miniaturized from the milli- to the microscale. Based on this advantageous scaling, we have adapted the technique demonstrated by Whitesides' group to apply it to microscopic silicon part-to-substrate assembly.

II. MICROASSEMBLY USING CAPILLARY FORCES

The self-assembly technique described in this paper is summarized in Fig. 1. In our process, the part and substrate binding sites are complementary, photolithographically defined shapes that need not cover the entire face surface of the part. To prevent the microscopic parts from binding to each other in solution via capillary forces, only the substrate binding sites are lubricated in our process. In order to create hydrophobic binding sites on the part and substrate surfaces, evaporated gold shapes are patterned and self-assembled monolayers
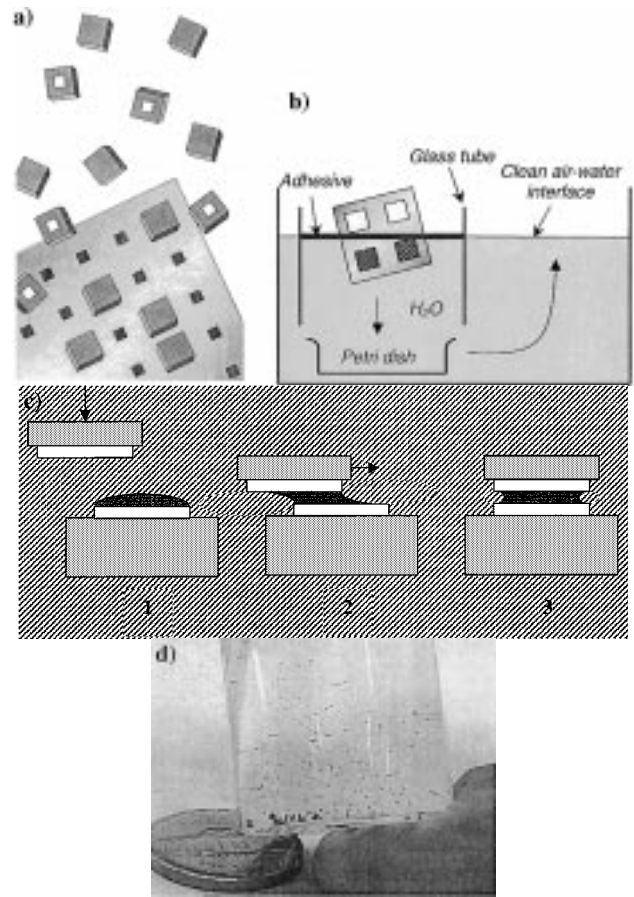

Fig. 1. (a) Schematic of fluidic self-assembly technique. (b) Substrate adhesive-coating procedure, adapted from [16]. (c) Self-assembly using capillary forces of the adhesive. (d) Photograph of assembly test parts in a vial of water.

(SAMs) are deposited on them using alkanethiol precursor molecules. The gold regions are thereby rendered hydrophobic, while the remaining silicon or quartz areas are silicon-dioxide coated and hydrophilic. Then, the substrate is passed through a film of hydrophobic liquid adhesive on water, causing this hydrocarbon to selectively coat the binding sites [Fig. 1(b)], as shown in [16] in the context of polymer microlenses. The microscopic parts are then directed toward the substrate surface under water using a pipette, as depicted in Fig. 1(a). Once the hydrophobic pattern on a part comes into contact with an adhesive-coated substrate binding site, shape matching occurs spontaneously due to interfacial free energy minimization of the adhesive-water and SAM-water interfaces [Fig. 1(c)]. The assembled parts are held in place under water by the capillary forces of the adhesive, and permanent bonding is achieved by curing the adhesive using heat or ultraviolet light.

This assembly technique can give submicrometer alignment precision since the positioning depends on the resolution of the patterned hydrophobic shapes. While we have demonstrated this technique using SAMs on patterned gold-on-silicon and quartz substrates, many other strategies for patterning surfaces at the microscale exist in the literature, including ultraviolet exposure of SAMs [17], microcontact printing of one type of SAMs and subsequent exposure to a second set of SAMs [18], [19], patterning and selective removal of polymer films [20], and O$_2$

TABLE I
DIMENSIONS AND SHAPES OF BINDING SITES AND TEST PARTS USED IN
SELF-ASSEMBLY EXPERIMENTS

Binding Site Shape	Binding Site Dimensions	Part Dimensions
⬤	$d = 100, 195\ \mu m$	$d = 200\ \mu m$
⬡	$d = 200\ \mu m$	$d = 464\ \mu m$
▢	$l = 20, 40, 150\ \mu m$	$l = 150\ \mu m$
	$l = 200, 380, 400\ \mu m$	$l = 400\ \mu m$
▭	$l = 500\ \mu m$ $w = 250\ \mu m$	$l = 500\ \mu m$ $w = 250\ \mu m$
◖	$d = 300\ \mu m$	*square*, $l = 400\ \mu m$
⌇	$l = 327\ \mu m$ $w = 253.5\ \mu m$	*square*, $l = 400\ \mu m$

plasma exposure of polymer films with a masking layer [21]. The general microassembly approach described here requires surface modification but does not necessitate bulk micromachining of the substrate or place shape constraints on the microcomponents. Therefore, it may be applied to parts and substrates prepared using most micromachining techniques and including materials such as semiconductors, metals, glass, and plastics. Also, since the binding site need not cover an entire face of the micropart, there is more flexibility in design of the part, and the adhesive thickness, which depends on the dimensions of the binding site, can be specified. Finally, this assembly technique is applicable to a wide range of part sizes due to the relative strength of capillary forces from the milli- down to the nanoscale.

III. EXPERIMENTAL METHODS

A. Design and Fabrication

We conducted experiments using two types of binding site shapes—polygons with in-plane rotational symmetry and closed shapes without in-plane rotational symmetry. The first group of binding site shapes includes regular hexagons, squares, rectangles with an aspect ratio of two, and twenty-gons (approximately circles). Shapes without in-plane rotational symmetry—semicircles and commas—were used to test the orientational selectivity of this assembly technique. The dimensions of the binding sites and test parts are given in Table I. These dimensions were chosen for two reasons—first, the binding site surface areas and the resulting adhesive drop volumes are within the range where capillary forces dominate over gravitational and shear forces. Second, parts of this size are easily observable by eye and optical microscopy.

The silicon test parts with gold patterns on one face were fabricated from silicon-on-insulator wafers with Si (100) layer thicknesses of 15 and 50 μm (Bondtronix and BCO Technologies). The part shapes were defined using deep reactive ion etching in a Surface Technology Systems silicon etcher with 1–2 μm of patterned I-line photoresist (Arch Chemicals) as the masking layer. After photoresist removal in PRS-3000 Positive Resist Stripper (J. T. Baker) at 90 °C, SJR 5740 photoresist (Shipley) was applied to be used as a thick lift-off layer for

gold/chrome patterning. The photoresist was spun on at 350 rpm for 30 s, followed by 15 s at 3500 rpm; the wafers were then baked at 115 °C for 7 min. After photolithography and developing in Microposit Concentrate (Shipley) for 4 min, thermal evaporation was used to coat the wafers with 10 nm of chrome as an adhesion layer and 50 nm of gold. The photoresist was dissolved in acetone, and the wafer was briefly ultrasonicated and rinsed in methanol. Photoresist residue was removed by immersion for 10 min in PRS-3000 at 90 °C.

The alignment precision afforded by this assembly technique was measured using test parts and binding site patterns with vernier scales of 0.2 μm resolution. To eliminate the photolithographic contribution of layer-to-layer misalignment, the vernier scales on the parts and substrates were included in the masks used to define the gold binding sites. We used quartz substrates so that the alignment precision could be determined by turning the assembly over and taking photographs through the transparent substrate. These photographs were then analyzed using Matlab line scans to determine the misalignment.

In order to etch the sacrificial silicon dioxide layer and release the microparts into solution, the chips are immersed in concentrated hydrofluoric acid (HF, 49%) in a Teflon dish. HF etching renders the silicon surfaces of the blocks and the handle chip hydrophobic, and the parts are attracted to the handle chips when the oxide etching is complete due to hydrophobic interactions [22]. The chips, which have released parts on their surfaces, are then transferred to a clean glass vial filled with methanol; the parts are carefully rinsed with fresh methanol using successive dilutions to remove residual traces of HF. The alcohol wets the hydrophobic silicon surfaces, and the microparts are released into the liquid upon agitation. All glassware is cleaned in a 4:1 (vol.) solution of concentrated H_2SO_4: 30% H_2O_2 for 20 min and rinsed in deionized water prior to use.

The silicon (100) (Wacker Siltronic) and quartz (Hoya) substrates used in the assembly experiments were prepared either by the lift-off procedure described earlier or by evaporating gold/chrome films onto the wafers, photolithographically patterning the films into the desired shapes, and etching with gold and chrome etch solutions (Gold Etchant Type TFA, Transene Company; and Cr-7 Chromium Photomask Etchant, Cyantek Corporation). The lift-off process was used exclusively to pattern binding sites with features smaller than 25 μm.

B. Surface Treatment

The SAM solution is 1 mM 1-octadecanethiol ($CH_3(CH_2)_{17}SH$, 98%, Aldrich) in absolute ethanol (Aaper). The parts stored in methanol are first rinsed with water and then allowed to soak in 30% H_2O_2 for 15 min to reoxidize the silicon surfaces and render them hydrophilic, as well as clean the gold regions. Next, the parts are rinsed in pure ethanol; the ethanol is drained and the vial is filled with the SAM solution. The parts and substrate chips are immersed in the solution for 24 h silicon (100), and gold/chrome-coated silicon chips are included to monitor the surface conditions. Once the monolayers are formed, the parts and substrate chips are rinsed several times with ethanol and stored in methanol. Contact angle measurements on monitor chips were performed using a Krüss goniometer with water and hexadecane. In addition,

contact angle measurements using hexadecane on monitor surfaces submerged in water were also taken.

C. Self-Assembly

A schematic of the substrate adhesive-coating process as demonstrated in [16] is shown in Fig. 1(b). A glass dish is half-filled with water, a smaller glass dish is submerged within it, and a glass cylinder is placed above the smaller dish. A substrate chip is removed from storage in methanol and dried using nitrogen. A 50-μL drop of the adhesive (compositions of the photo- and heat-curable methacrylate mixtures are described in the next section) is applied to the surface of the water located within the glass cylinder. Next, the chip is lowered through the hydrocarbon-water interface at a speed of ~1 cm/s to rest in the small glass dish. As the chip passes into the water, adhesive droplets assemble only on the hydrophobic SAM-coated regions. The small dish containing the adhesive-coated substrate is then moved away from the cylinder and removed from the larger dish. This ensures that the substrate remains submerged in water throughout the process and the surface of the water in the small dish is not contaminated by a hydrocarbon film.

Next, the methanol in the vial containing the microparts is replaced with water. This is done carefully to prevent the parts from reaching the air–water interface where they would float, hydrophobic side facing up, if the binding site area is a sufficiently large fraction of the face area. The parts are drawn into a clean glass pipette and delivered to the submerged substrate surface; unbound parts are removed using a gentle stream of flowing water and recycled. Optical microscope photographs were taken to assess assembly yield, alignment yield, and precision. Video clips of self-assembly events were digitized using Adobe Premiere software.

D. Adhesive Bonding

Bonding to the quartz substrate was accomplished using a photopolymerizable acrylate adhesive, as in [23]. This mixture consists of 96 wt.% n-dodecyl methcrylate monomer (Alfa Aesar), 2 wt.% 1.6-hexanediol diacrylate (Aldrich) as crosslinker and 2 wt.% benzoin methyl ether (Aldrich) as photoinitiator (viscosity of mixture $\approx$ 5 cp). The adhesive was polymerized by turning the assembly over in water and exposing the reverse side of the substrate to ultraviolet light at an intensity of 15 mW/cm^2 for 1 h (Spectronics, SB-100P). The substrate was submerged in ~5 mm of water. Prior to light exposure, nitrogen was bubbled through the water to reduce the dissolved oxygen concentration since oxygen is known to have an inhibitory effect on this polymerization reaction.

A heat-curable version of the adhesive mixture was employed for bonding to opaque substrates. This mixture is composed of 85 wt.% n-dodecyl methacrylate monomer, 14.5 wt.% triethyleneglycol dimethacrylate (Electron Microscopy Sciences) as crosslinker and 0.5 wt.% benzoyl peroxide (Aldrich) as thermal initiator (viscosity of mixture $\approx$ 1 cp). Here, the adhesive was hardened by immersing the assembly in a water bath at 80 °C for 16 h. Nitrogen was bubbled continuously through the water bath to reduce the dissolved oxygen concentration. The alignment precision after adhesive hardening was measured
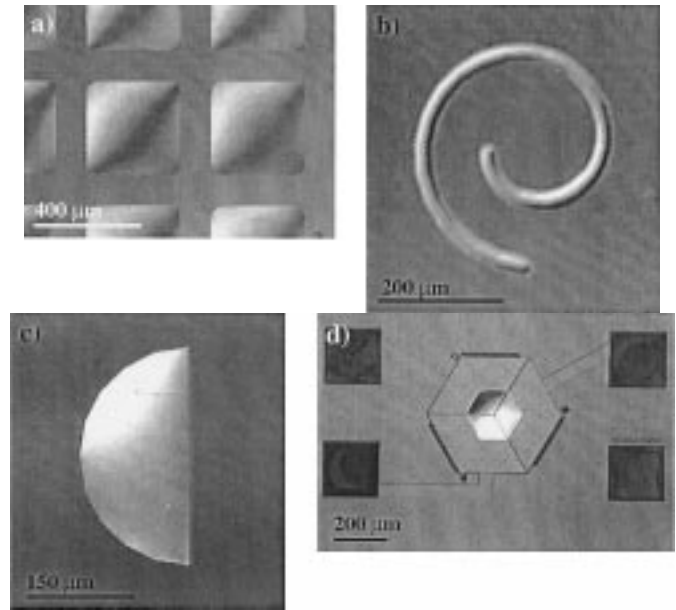

Fig. 2. Photographs taken under water of adhesive droplets wetting hydrophobic patterns on quartz and silicon substrates: (a) squares on quartz, (b) spiral on silicon, (c) semicircle on silicon, and (d) hexagon on a surface micromachined actuator on silicon.

using the parts and substrates with vernier scales. Stroboscopic interferometry was employed to quantify the tilt and flatness of the assembled and bonded parts.

IV. RESULTS AND DISCUSSION

A. Surface Treatment

Immersion of clean gold/chrome coated silicon test pieces in the alkanethiol solution results in the formation of a well-packed hydrophobic monolayer, as confirmed by water and hexadecane contact angles of 111 and 47°, respectively [24]. In a water environment, hexadecane droplets wet this hydrophobic surface with a contact angle of 30°. Wetting occurs because the free energy of the hexadecane-SAM interface is lower than that of the SAM-water interface. In contrast, hexadecane does not wet the hydrophilic oxidized silicon surfaces in water, as confirmed by a contact angle of 180°. Here, the free energy of the hexadecane-SiO$_2$ interface is higher than that of water-SiO$_2$. The wetting behavior of hexadecane on these hydrophobic and hydrophilic surfaces is similar to that of the hydrocarbon adhesives used in the assembly experiments, since both liquids are mainly composed of CH$_2$ units.

Once the patterned gold-silicon and gold-quartz substrates were treated with the SAM solution, the gold regions were made hydrophobic while the oxide-coated silicon or quartz areas remained hydrophilic. When a patterned substrate is lowered through the adhesive–water interface, the adhesive does not wet the hydrophilic regions but does form self-assembled droplets on the hydrophobic regions. In Fig. 2, droplets of the methacrylate adhesive can be seen wetting hydrophobic patterns under water. This results from the minimization of interfacial liquid energies, since the energetic cost of the methacrylate next to the SAM is lower than that of water bordering the more hydrophobic methyl groups of the SAM.

The droplet dimensions are determined by several factors including the shape and area of the hydrophobic regions, the receding contact angle of the adhesive on the SAM in water, the adhesive viscosity, and the speed of substrate lowering. [14], [16]. Due to the small sizes involved, the droplet dimensions are not significantly affected by the adhesive buoyancy in water. Measurements on side profile microscope images of the heat-curable adhesive droplets on circular sites (diameter 195 μm) gave a center height of ~17 μm and a contact angle of ~20°. If the shape of the adhesive droplet is assumed to be a spherical cap with the appropriate contact angle, the predicted adhesive volume is calculated as ~0.48 nL. This liquid layer provides the means for lubrication, self-alignment, and bonding in the assembly experiments, as in [11] and [23].

Once the surface treatment was completed, we stored the released parts and substrates in methanol. Alcohol was used instead of water because its interfacial energy with the SAM is low, and, therefore, the adsorption of contaminants onto the SAMs from solution is not favored. Also, we did not store the substrate chips in air due to the high surface energy of the clean silicon dioxide regions, which would favor the adsorption of organic contaminants and make the regions hydrophobic more quickly over time.

We observed that the cleanliness of the glass vials used to store the released parts was important. If the glassware was not cleaned with the piranha solution, the binding sites on the microscopic parts adhered to any hydrophobic regions on the glass when the alcohol was replaced with water for the self-assembly step. This adhesion is probably due to hydrophobic attractions in water.

B. Self-Assembly

In the assembly experiments, we observed that the hydrophilic silicon sides of the parts do not adhere to either the hydrophobic or hydrophilic regions of the substrate. In contrast, when the hydrophobic gold binding site on a part comes into contact with a matching adhesive-coated pattern on the substrate, self-alignment occurs. This behavior is due to the spontaneous wetting of the part binding site by the adhesive and the strong restoring forces exerted by the adhesive capillary between the part and substrate binding sites in water. The adhesive layer acts as a lubricant, facilitating movement of the part so the amount of SAM and adhesive surface area in contact with water is cooperatively minimized, thereby minimizing the interfacial free energy of the system [11]. This spontaneous shape matching occurs within 1 s; increasing the viscosity of the adhesive has been shown to slow the self-alignment step. Fig. 3 contains frames of a self-assembly event from a video taken at a microscope.

Once assembled, a part does not become unstuck at the level of agitation required to move the unbound parts over the substrate or when the substrate is turned upside down. For a self-assembled disk with binding site of diameter 200 μm, we have estimated that a force on the order of 10^{-4} N is required to overcome the capillary "bond" in the z-direction [14]. This is compared to drag and gravitational forces on the order of 10^{-7} and 10^{-8} N, respectively. Therefore, with a constant supply of parts,
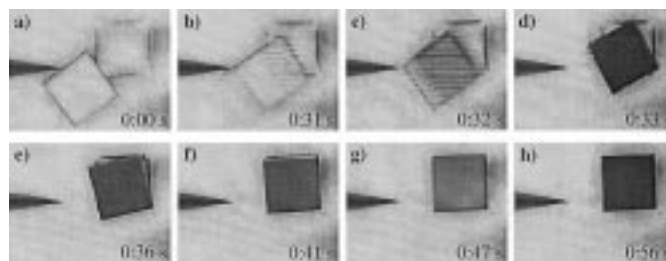

Fig. 3. Frames of a self-assembly event from a video taken at a microscope: binding sites make contact at (a) 0:00 s, (b) 0:31 s, (c) 0:32 s, (d) 0:33 s, (e) 0:36 s, (f) 0:41 s, (g) 0:47 s, and (h) self-alignment at 0:56 s. Part dimensions are 400 × 400 × 15 μm³.
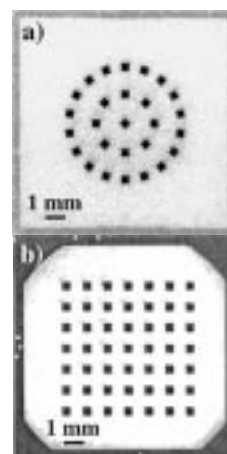

Fig. 4. Arrays of square parts on quartz substrates in (a) ring and (b) grid configurations.

it should be possible to rapidly assemble large arrays with high yield. We have assembled 98-part arrays in less than 1 min with no defects; self-assembled arrays of square parts in two configurations are pictured in Fig. 4.

An alignment yield of 100% was observed for the polygon binding sites—squares, regular hexagons, circles, and rectangles of aspect ratio 2. The micrographs in Fig. 5(a) and (b) show parts self-assembled in water using circular and hexagonal binding sites. We also varied the fraction of binding site area on the part face, as summarized in Table I. Self-assembly was successful using square sites as small as 20 × 20 μm², or 1.8% of the face surface area on a 150 × 150 × 50 μm³ part [Fig. 5(c)]. In theory, smaller sites may be used but would necessitate a higher concentration of parts in solution, greater mobility of parts on the substrate, or longer assembly times to increase the probability of contact between part and substrate binding sites. Experiments using parts and substrates with vernier scales indicate that square binding sites give an alignment precision of ≤ 0.2 μm as-assembled in water. Fig. 6(a) shows a photograph of a self-assembled part taken through the reverse side of the quartz substrate and a closeup of the part-substrate vernier scales.

Binding sites without in-plane rotational symmetry, semicircles and commas, gave alignment yields of approximately 30–40%. Fig. 7 contains micrographs of aligned and misaligned parts with these binding sites shapes. The low alignment yield may be due to the presence of a local interfacial energy
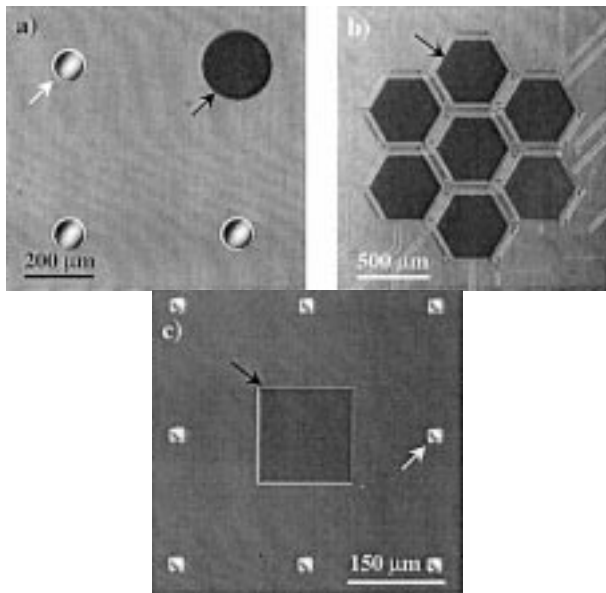
Fig. 5. Self-assembly of test parts onto patterned adhesive-coated sites on silicon substrates under water: (a) circular part, (b) hexagonal parts on micromachined actuators, and (c) square part. Black arrows indicate assembled parts and white arrows point to unoccupied substrate sites. Binding site in (c) is 1.8% of the part face area. Assembled parts appear darker due to use of Nomarski interference.
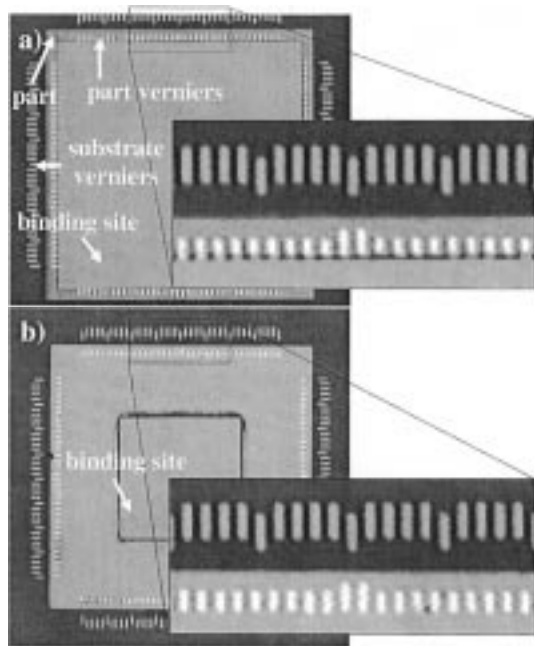

Fig. 6. (a) Part-to-substrate self-assembly in water with vernier scales to measure alignment precision, seen through the reverse side of quartz substrate. The binding site is $400 \times 400 \, \mu\text{m}^2$. Closeup of part-substrate vernier alignment shows alignment precision is $\leq 0.2 \, \mu\text{m}$. (b) Rotational shift after activating adhesive on a $200 \times 200 \, \mu\text{m}^2$ binding site is within $1.2 \, \mu\text{m}$, or $\sim 0.3°$, as shown by magnified view.

minimum at a rotational misalignment of $180°$ and further decreased by the vernier scales. Also, we measured an alignment precision of less than $1 \, \mu\text{m}$ for these shapes. A possible reason for this reduced precision may be that the energy minimum is less sharp for these shapes than for the polygons. These results
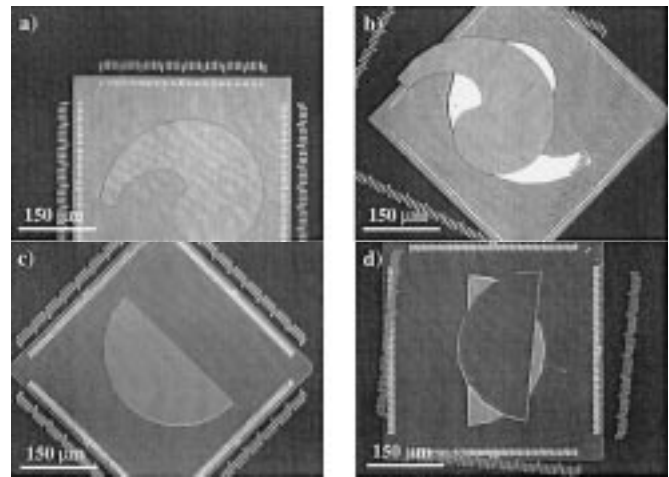

Fig. 7. Optical micrographs taken through quartz substrates of silicon parts assembled using binding sites without a rotational symmetry axis in water: (a) comma-shaped site, aligned; (b) comma-shaped site, misaligned; (c) semicircle site, aligned; and (d) semicircle site, misaligned.
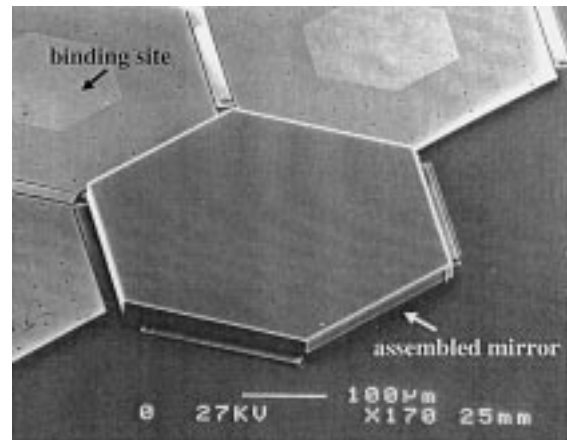

Fig. 8. SEM of self-assembled and bonded single-crystalline silicon mirror on released actuator.

indicate that further work must be done in binding site shape selection in order to achieve orientational selectivity [25].

If the binding sites on the parts were coated with the adhesive as well, we found that pairs of parts would bond to each other in water, as expected.

C. Adhesive Bonding

During the polymerization of the heat-curable adhesive, the parts shift slightly, probably due to nonuniform curing of the adhesive and the resultant stresses. Using vernier scales on the parts and substrates, the alignment precision was measured as less than $1.2 \, \mu\text{m}$ of rotational shift, or $\theta < 0.31°$. Stroboscopic interferometry studies show that the heat-curable adhesive formula and curing schedule result in minimal warpage of the silicon microparts. For a 15-μm-thick part, the curvature is less than 100 nm over a square binding site $400 \, \mu$m on a side. This warpage is reduced to less than 16 nm over a 15-μm-thick hexagonal mirror $464 \, \mu$m in diameter with a hexagonal binding site $200 \, \mu$m in diameter, giving a radius of curvature of ~ 1.25 m. The tilt was measured as approximately

300 nm over 50-μm-thick parts with circular binding sites 200 μm in diameter, corresponding to an angle of 0.09°. This tilt may be reduced further by adding mechanical features to the parts or substrates to define planarity.

We used this self-assembly technique to position single-crystalline silicon micromirrors onto surface micromachined actuators for improved reflectivity and flatness in an adaptive optics application [26]. By decoupling mirror fabrication from the actuator fabrication process, each process can be optimized independently of the other, and the requirement for extremely low stress and stress-gradient films for the actuators is relaxed. The mirrors were self-assembled and bonded before the actuators were released using HF, and the adhesive withstood the release process. Finally, the assembly was dried with carbon dioxide critical point drying. Fig. 8 shows an SEM micrograph of a hexagonal mirror self-assembled and bonded on a released actuator.

V. SUMMARY AND CONCLUSIONS

We have demonstrated a fluidic technique based on patterned shapes of hydrophobic SAMs and capillary forces to self-assemble microfabricated silicon blocks onto silicon and quartz substrates. Here, the driving force for self-assembly is the minimization of the interfacial free energy of the system; self-alignment to an adhesive-coated binding site occurs within a second of contact for regular polygonal binding sites. The assembly is then made permanent by activating the adhesive using ultraviolet light or heat. The alignment precision afforded by square binding sites is less than 0.2 μm as-assembled in water, and a rotational misalignment of less than $\sim$0.3° was measured after adhesive hardening. This assembly approach offers three main advantages over existing assembly methods—it gives high alignment precision, there is a great deal of flexibility in the choice of part and substrate materials, and it does not require bulk micromachining of the substrate. Using rectangular binding sites of an aspect ratio of two, parts self-assemble to matching substrate sites in two possible orientations. In order to give unique orientational selectivity, this assembly technique may be used in conjunction with three-dimensional shape complementarity of the part and substrate sites.

In current work, we are using the public-domain finite-element program *Surface Evolver*[1] to model the self-assembly using surface energy parameters and energy minimization. This model will aid in understanding the dynamics of the self-assembly and in the optimization of the binding site shape [25]. Establishing part-substrate electrical connections following self-assembly is an important direction for future research. Also, the development of a part reflow system with several part delivery lines should allow the assembly of large arrays consisting of thousands to millions of parts with extremely high yield [6].

It is predicted that self-assembly techniques such as the one described here will form an enabling technology for MEMS due to their versatility and economic advantages. Possible applications include the assembly of mirrors onto actuator arrays for adaptive optics, lasers, and photodeterctors onto microfluidic chips for use in biochemical detection, and optical elements onto microactuator chips for optical communication.

REFERENCES

[1] M. B. Cohn, K. F. Böhringer, J. M. Noworolski, A. Singh, C. G. Keller, K. Y. Goldberg, and R. T. Howe, "Microassembly technologies for MEMS," in *Proc. SPIE Micromachining and Microfabrication*, Santa Clara, CA, Sept. 20–22, 1998, pp. 2–16.

[2] C. G. Keller and R. T. Howe, "Hexsil tweezers for teleoperated micro-assembly," in *Proc. 1997 Int. Workshop Micro Electro Mechanical Systems*, Nagoya, Japan, Jan. 26–30, 1997, pp. 72–77.

[3] A. Singh, D. A. Horsley, M. B. Cohn, A. P. Pisano, and R. T. Howe, "Batch transfer of microstructures using flip-chip solder bump bonding," in *Proc. 1997 Int. Conf. Solid-State Sensors and Actuators*, Chicago, IL, June 16–19, 1997, pp. 265–268.

[4] A. S. Holmes and S. M. Saidam, "Sacrificial layer process with laser-driven release for batch assembly operations," *J. Microelectromech. Syst.*, vol. 7, pp. 416–422, 1998.

[5] H.-J. J. Yeh and J. S. Smith, "Fluidic assembly for the integration of GaAs light-emitting diodes on Si substrates," *IEEE Photon. Technol. Lett.*, vol. 6, pp. 706–708, 1994.

[6] Alien Technology, Morgan Hill, CA, http://www.alientechnology.com/technology/overview.html..

[7] T. Nakakubo and I. Shimoyama, "Three-dimensional micro self-assembly using bridging flocculation," in *Proc. 1999 Int. Conf. Solid-State Sensors and Actuators*, Sendai, Japan, June 7–10, 1999, pp. 1166–1169.

[8] Y. Murakami, K. Idegami, H. Nagai, A. Yamamura, K. Yokoyama, and E. Tamiya, "Random fluidic self-assembly of microfabricated metal particles," in *Proc. 1999 Int. Conf. Solid-State Sensors and Actuators*, Sendai, Japan, June 7–10, 1999, pp. 1108–1111.

[9] M. B. Cohn, "Assembly Techniques for Microelectromechanical Systems," Ph.D. dissertation, Univ. of California at Berkeley, 1997.

[10] K.-F. Böhringer, K. Goldberg, M. Cohn, R. T. Howe, and A. P. Pisano, "Parallel microassembly with electrostatic force fields," in *Proc. 1998 IEEE Int. Conf. Robotics & Automation*, Leuven, Belgium, May 1998, pp. 1204–1211.

[11] A. Terfort, N. Bowden, and G. M. Whitesides, "Three-dimensional self-assembly of millimeter-scale components," *Nature*, vol. 386, pp. 162–164, 1997.

[12] J. Tien, T. L. Breen, and G. M. Whitesides, "Crystallization of millimeter-scale objects with use of capillary forces," *J. Amer. Chem. Soc.*, vol. 120, pp. 12 670–12 671, 1998.

[13] T. L. Breen, J. Tien, S. R. J. Oliver, T. Hadzic, and G. M. Whitesides, "Design and self-assembly of open, regular, 3D mesostructures," *Science*, vol. 284, pp. 948–951, 1999.

[14] A. W. Adamson and A. P. Gast, *Physical Chemistry of Surfaces*. New York: Wiley, 1997.

[15] W. S. N. Trimmer, "Microrobots and micromechanical systems," *Sensors Actuators*, vol. 19, pp. 267–287, 1989.

[16] H. A. Biebuyck and G. M. Whitesides, "Self-organization of organic liquids on patterned self-assembled monolayers of alkanethiolates on gold," *Langmuir*, vol. 10, pp. 2790–2793, 1994.

[17] J. Huang, D. A. Dahlgren, and J. C. Hemminger, "Photopatterning of self-assembled alkanethiolate monolayers on gold: A simple monolayer photoresist utilizing aqueous chemistry," *Langmuir*, vol. 10, pp. 626–628, 1994.

[18] A. Kumar, H. A. Biebuyck, and G. M. Whitesides, "Patterning self-assembled monolayers: Applications in materials science," *Langmuir*, vol. 10, pp. 1498–1511, 1994.

[19] D. Qin, Y. Xia, B. Xu, H. Yang, C. Zhu, and G. M. Whitesides, "Fabrication of ordered two-dimensional arrays of micro- and nanoparticles using patterned self-assembled monolayers as templates," *Adv. Mater.*, vol. 11, pp. 1433–1437, 1999.

[1]See http://www.susqu.edu/facstaff/b/brakke/evolver.html.

[20] P. F. Man, C. H. Mastrangelo, M. A. Burns, and D. T. Burke, "Microfabricated plastic capillary systems with photo-definable hydrophilic and hydrophobic regions," in *Proc. 1999 Int. Conf. Solid-State Sensors and Actuators*, Sendai, Japan, June 7–10, pp. 738–741.

[21] L. P. Lee, "Key elements of biomedical polymer optoelectromechanical systems," Ph.D. dissertation, Univ. of California at Berkeley, 2000.

[22] J. Israelachvili, *Intermolecular and Surface Forces, With Applications to Colloidal and Biological Systems*. London, U.K.: Academic, 1985.

[23] A. Terfort and G. M. Whitesides, "Self-assembly of an operating electrical circuit based on shape complementarity and the hydrophobic effects," *Adv. Mater.*, vol. 10, pp. 470–473, 1998.

[24] A. Ulman, *Introduction to Ultrathin Organic Films: From Langmuir-Blodgett to Self-Assembly*. San Diego, CA: Academic, 1991.

[25] K. F. Böhringer, U. Srinivasan, and R. T. Howe, "Modeling of capillary forces and binding sites for fluidic self-assembly," in *Proc. 14th Int. Conf. Micro Electro Mechanical Systems*, Interlaken, Switzerland, Jan. 21–25, 2001.

[26] U. Srinivasan, M. H. Helmbrecht, C. Rembe, R. S. Muller, and R. T. Howe, "Fluidic self-assembly of micromirrors onto surface micromachined actuators," in *2000 IEEE/LEOS Intl. Conf. Optical MEMS*, Kauai, HI, Aug. 21–24, pp. 59–60.

Dorian Liepmann received the B.S. and M.S. in chemical engineering from the California Institute of Technology, Pasadena, and the Ph.D. degree from the University of California, San Diego.

He worked in the Advanced Technology Group at SAIC, La Jolla, CA, on projects for the U.S. Navy. Previously, he was a Member of the Arroyo Center, providing technology and policy analysis for the Army. He joined the Mechanical Engineering Department at the University of California at Berkeley in 1993 and the Bioengineering Department in 1999, in which he is currently Vice Chair. He is an Associate Director of the Berkeley Sensor & Actuator Center. His research interests include microfluid dynamics, mixing, transition, and vortex dynamics. He is currently working on the application of MEMS to biological and medical problems.

Roger T. Howe (S'79–M'84–SM'93–F'96) received the B.S. degree in physics from Harvey Mudd College, Claremont, CA, in 1979 and the M.S. and Ph.D. degrees in electrical engineering from the University of California at Berkeley in 1981 and 1984.

He was a member of the Faculty of Carnegie-Mellon University, Pittsburgh, PA, during the 1984–1985 academic year and was an Assistant Professor at the Massachusetts Institute of Technology, Cambridge, from 1985 to 1987. In 1987, he joined the Department of Electrical Engineering and Computer Sciences at the University of California at Berkeley, where he is now a Professor as well as a Director of the Berkeley Sensor & Actuator Center. In 1997, he became a Professor in the Department of Mechanical Engineering. His research interests include microelectromechanical system design, micromachining processes, and massively parallel assembly processes. He is a coauthor (with C. G. Sodini) of *Microelectronics: An Integrated Approach* (Englewood Cliffs, NJ: Prentice-Hall, 1997).

Prof. Howe was Co-General Chairman of the 1990 IEEE Micro Electro Mechanical Systems Workshop (MEMS'90) and General Chairman of the 1996 Solid-State Sensor and Actuator Workshop at Hilton Head, SC. He was a Corecipient (with R. S. Muller) of the 1998 IEEE Cledo Brunetti Award "for leadership and pioneering contributions to the field of microelectromechanical systems." He is an Editor of the IEEE JOURNAL OF MICROELECTROMECHANICAL SYSTEMS.

Uthara Srinivasan received the B.S. degree in chemical engineering with a certificate in materials science from Princeton University, Princeton, NJ, in 1995. She is currently pursuing the Ph.D. degree in chemical engineering at the University of California at Berkeley.

Her research interests include the application of self-assembly processes and surface patterning using self-assembled monolayers to MEMS and bio-MEMS.